# Sorption of tryalkoxysilane in low-cost porous silicates using a supercritical $CO_2$ method

P. López-Aranguren[1,3], J. Saurina[2], L.F. Vega[3,4], C. Domingo[1,*]
[1]*Instituto de Ciencia de Materiales de Barcelona (ICMAB-CSIC), Campus de la UAB, 08193 Bellaterra, Spain. E-mail: conchi@icmab.es*
[2]*Department of Analytical Chemistry. University of Barcelona, Martí I Franquès 1 – 11, 08028 Barcelona, Spain.*
[3]*MATGAS Research Center, Campus de la UAB s/n, 08193 Bellaterra, Spain.*
[4]*Carburos Metálicos, Air Products Group, C/ Aragón 300, 08009 Barcelona, Spain.*

## ABSTRACT

Trialcoxysilanes are bifunctional molecules widely used to obtain self-assembled coatings by the chemisorption route in liquid solvents. However, problems arise when the method is used for porous materials due to cross-linking of alkylsilanes in solution, which lead to multilayer deposition, non-uniform surface coverage and pore blocking. In previous works, we have reported detailed studies of the bottom-up formation of hybrid materials by the self-assembly of trialkoxysilanes on the surface of nanoparticulate systems using supercritical $CO_2$ ($scCO_2$). In this study, the supercritical silanization process is extended to the modification of the internal surface of mesoporous silica gels. The amorphous mesoporous supports were chosen for analysis in front of the most studied ordered mesoporous silicas of the type MCM-41 or SBA-15, because amorphous silica materials are considered low-cost adsorbents and could be used in a large amount of bulk applications. A hydrophobic silane was used to impregnate the internal surface to obtain oil adsorbents.

**Key words**: supercritical, silanization, mesoporous, microporous, water adsorption.

## INTRODUCTION

A simple and cost-effective way of regularly organize chemical entities on functional surfaces is represented by their self-assembly [1]. One of the most successful self-assembly approach is the chemical grafting of long hydrocarbon chains (R) on hydrated surfaces *via* trifunctional silanes, most typically, trimethoxy R-Si$(MeOH)_3$ or triethoxy R-Si$(EtOH)_3$ [2-4], forming well-ordered monolayers. Disadvantages of the chemisorption route include the necessity of applying large volumes of water, alcohols and other organic together with nanoparticles and nanopores may be complicated due to cross-linking of alkylsilanes in solution, multilayer deposition, non-uniform surface coverage and pore blocking [5-11].

It has been long-established that supercritical fluids can be used to design innovative processes by taking advantage of both physical and chemical fabrication approaches, which could be applied to the silanization process [12-17]. In previous works, we have reported detailed studies of the bottom-up formation of hybrid materials by the self-assembly of trialkoxysilanes on the surface of nanoparticulate systems using supercritical $CO_2$ ($scCO_2$) as the solvent medium [18-20]. In this study, the supercritical silanization process is extended to the modification of the internal surface of porous substrates, mainly silica derivatives, of diverse pore architecture. Two different silicium-based materials were scrutinized in this work belonging to diverse groups of porous solids: mesoporous silica gel ($SiO_2$) and microporous

aluminosilicates. Hydrophilic mesoporous silica gels are extremely important commercial substances, while organically modified silica gel (ormosil) is a class of novel material designed to host a large variety of organic and inorganic guests for applications in chromatography, catalysis, photochemistry, etc [21]. The choice of such amorphous silica materials relied on their low cost and adsorbent properties that are suitable for a large amount of bulk applications. A tridirectional zeolite Y, from the Faujasite class, was chosen as the microporous substrate [22].The thermal stability, surface coverage, pore structure and type of silane-silica interaction were determined using Fourier transformed infrared spectroscopy, thermogravimetric analysis and low-temperature $N_2$ adsorption-desorption characterization techniques. A Karl Fischer titration method was applied to quantify the adsorbed water content for both raw and silanized samples, thus giving an indication of hydrophilic modification [23].

## MATERIALS AND METHODS

### Materials

Some important characteristics of the processed matrices are shown in Table 1.

**Table 1.** Matrices characteristics.

| Type | Substrate | Sample | Supplier | $SiO_2$ [wt%] | Particle size [μm] | $V_p$ [$cm^3g^{-1}$] | $D_p$ [nm] |
|---|---|---|---|---|---|---|---|
| Mesoporous | Silica Blue | SB | Fluka | >99.8 | 1000-3000 | 0.1 | 2 |
| Microporous | Zeolite Y | ZY | Strem Chemicals | 49 | 20-50 | 0.05 | 1.3* |

* The zeolite Y architecture is defined as almost spherical cavities of 1.3 nm in diameter accessible through tetrahedral windows of 0.74 nm arranged in a tridirectional ordered structure [18].

The sample of amorphous silica gel (Silica Blue) has a mixture of meso and microporosity (SB, with cobalt chloride as indicator) and surface area in the order of 500-800 $m^2g^{-1}$. This material was partially dehydrated before use by heating it in an air oven at 120 ºC during 20 h. The crystalline aluminosilicate (ZY) has a tridirectional ordered pore structure. This zeolite was activated by calcination in a tubular oven (Carbolite 3216) at 520 ºC during 48 h under a flow of nitrogen with oxygen traces. The zeolite surface area after calcination was 740 $m^2g^{-1}$.

Octyltriethoxysilane ($C_8Si(OEt)_3$ from Fluka) and $CO_2$ (Carburos Metálicos S.A.) were used as solute and solvent, respectively. Reagents for $H_2O$ determination comprised Karl Fischer's Reagent composite (RV, 1 mL reagent ≈ 0.005 g $H_2O$) and methanol (RE, according to Karl Fischer), both from Panreac.

### Equipment and Procedure

The supercritical silanization of silica substrates was performed using the set-up depicted in Fig. 1. A high-pressure autoclave (TharDesign) with a volume of 100 mL, running in the batch mode, was used for silane deposition. A finger tight closure of Polyimide C cup-type ring containing a self-energizing spring was used to seal the reactor. Moreover, two single-crystal sapphire windows, placed 180º apart in the reactor body, allowed the visual follow-up of the process taking place inside of the reactor. The reactor was charged with *ca.*

0.5 g of substrate enclosed in a cylindrical cartridge made of 0.45 μm pore filter paper, which was placed in the upper part of the autoclave in a metallic support. Liquid silane (*ca.* 0.5 mL) was added to the bottom of the reactor. Experiments were performed in the batch mode. Liquefied $CO_2$ was compressed by a syringe pump (Teledyne ISCO-260 D) at the desired pressure (P). The autoclave was heated at the chosen temperature value (T) using electric resistances. The system was stirred at 300 rpm with a magnetic stirrer during the running time (t). At the end of each experiment, the reactor was depressurized and led to cool to room temperature. Recovered samples were washed with a continuous flow of $scCO_2$ at 10 MPa and 318 K during 30 min to remove the excess of deposited silane. For each substrate, a blank sample resulting from the supercritical treatment of the matrix in the absence of silane was also prepared under similar supercritical conditions of processing and washing.

**Characterization**

To confirm the presence of the coupling agent in the treated materials, Fourier transformed infrared (FTIR) spectra of the solid samples mixed with KBr were recorded on a Perkin-Elmer Spectrum One instrument. Thermogravimetric analysis (TGA) of the modified silicas was performed in Ar using a TGA PerkinElmer 7 and a heating rate of 10 $^{o}Cmin^{-1}$. Textural characteristics of blank and silanized $SiO_2$ substrates were studied by low-temperature $N_2$ adsorption-desorption analysis (ASAP 2000 Micromeritics). Prior to measurements, samples were dried at 150 ºC during 48 h. Specific surface area ($S_a$) was determined by the BET method. Mesopore volume ($V_p$) and mean pore diameter ($D_p$) were calculated using the BJH method from the adsorption branch of the isotherm, and micropore volume ($V_{mp}$) was estimated by the *t*-curve method. Weight loss data from the TGA of treated materials and specific surface area of blank substrates were used to further estimate the number of silane molecules per $nm^2$ [$ms/nm^2$] on the surface of the treated matrices. Molecular weight (Mw) calculations were performed independently for the trapped silanols ($Mw_{(C8Si(OH)3)}$ = 192) evaporated in the temperature interval 150-375 ºC, and grafted siloxane ($Mw_{(C8)}$ = 113) decomposed by cleavage of Si-C and C-C bond at temperatures higher than 375 ºC.

The adsorbed water content was measured using the Karl Fischer method. Silica porous samples were exposed to a relative humidity of 60-65 % (ambient conditions) at 21 ºC during 7 days. Samples were first dried at 120 ºC in an air oven during 20 h. At the used hydration temperature of 21 ºC, no significant hydrolysis of siloxane bonds was expected. The adsorbed water content was measured using a 633 Karl Fischer-Automat (Methrohm AG, Zofingen, Switzerland equipped with a 715 Dosimat burette and a 703 Ti Stand stirrer. Approximately 20 mg of each hydrated material was suspended in anhydrous methanol with the aid of magnetic stirring and titrated in a closed vessel using the Karl Fischer's reagent. Each sample was measured three times and the arithmetic mean was given as the adsorbed water value. Standard deviations < 5% were found. A sharp indication of the end point was obtained by amperometric detection. For the porous materials under study, the kinetics of water desorption were monitored at diverse preselected times of 2, 4, 6, 8, 10, 15, 20 and 30 min. The water desorption to the methanol phase was considered to be completed after this period.

## RESULTS AND DISCUSSION

A series of experiments were performed to evaluate the performance of the supercritical silanization method on porous substrates. Experimental conditions of each run are shown in Table 2, together with some products characteristics. The influence of the operating conditions (pressure between 100 and 200 bar, temperature between 45 and 75 ºC and reaction time between 90 and 240 min) on product characteristics was first evaluated. For the designed high-pressure procedure, the operating pressure and temperature determine the silane mole fraction in the fluid phase. Working conditions, specifically 100 bar and 75 ºC, corresponded to high solubility of silane in $scCO_2$ [24].

**Table 2**. Supercritical operating conditions and some obtained results: TGA estimated amount of deposited silane in the interval 150-600 ºC ($d_s$), some textural properties obtained by low temperature $N_2$ adsorption and adsorbed water ($A_w$), after 1 week of hydration at 60-65 % relative humidity.

| Sample | T [ºC] | P [bar] | t [min] | $d_s$ [$g_s g_m^{-1}$] | $S_a$ [$m^2 g^{-1}$] | $V_p$ [$m^3 g^{-1}$] | $V_{mp}$ [$m^3 g^{-1}$] | $A_w$ [%wt] |
|---|---|---|---|---|---|---|---|---|
| b-SB | 75 | 100 | 120 | - | 611 | 0.09 | 0.18 | 14.3 |
| 1-SB | 75 | 100 | 90 | 0.146 | 500 | 0.07 | 0.17 | |
| 2-SB | 75 | 100 | 240 | 0.144 | 382 | 0.06 | 0.10 | |
| 5-SB | 75 | 100 | 420 | 0.163 | 52 | 0.02 | 0.01 | 9.7 |
| 3-SB | 75 | 200 | 90 | 0.133 | 320 | 0.05 | 0.08 | |
| 4-SB | 45 | 200 | 120 | 0.132 | 464 | 0.07 | 0.13 | 2 |
| b-ZY | 75 | 100 | 120 | - | 600 | - | 0.28 | 19.0 |
| 2-ZY | 75 | 100 | 240 | 0.156 | 425 | - | 0.17 | |
| 5-ZY | 75 | 100 | 420 | 0.161 | 352 | - | 0.14 | |
| 3-ZY | 75 | 200 | 90 | 0.186 | 360 | - | 0.17 | |
| 4-ZY | 45 | 200 | 120 | 0.179 | 360 | - | 0.17 | 15.3 |

The reaction time is identified as a key parameter influencing the diffusion of the silane solution in the substrate pores. However, in the performed series of experiments, with reaction times ranging from 90 to 240 min, results indicated that the influence of the reaction time was quite limited, suggesting that the silanization process was not diffusion-controlled at the experimental conditions investigated. This finding is related to the facility of $scCO_2$ for fast diffusion to the interior of the porous networks. Only for the mesoporous SB sample, the amount of deposited silane increased in experiments performed during 420 min, but in these cases the effect was most likely associated to multilayer formation. On the other hand, large differences in regard of deposited silane and resulting sample characteristics were observed as a function of the used substrate.

**Deposited silane**

Thermal behavior of silane treated samples as well as the amount of impregnated silane was studied by thermogravimetric analysis (Fig. 2).

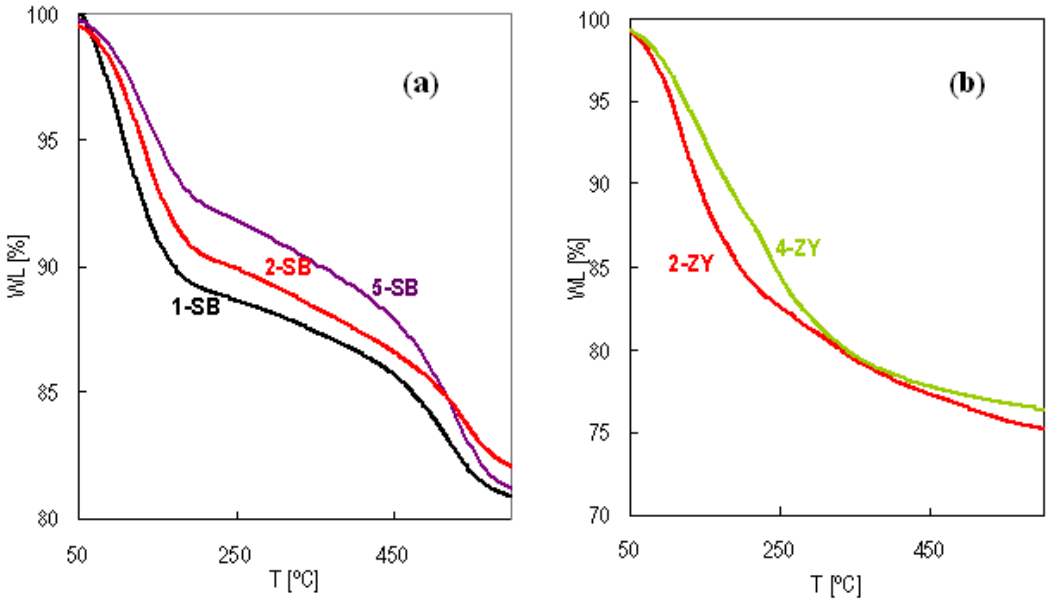


**Figure 2.** Selected TGA profiles of samples prepared using different conditions for: (a) SG, and (b) ZY.

For all alkylsilica samples prepared, the first significant weight loss occurred below *ca.* 150 ºC, and it was attributed to desorption of physically adsorbed water, also present in the raw substrates. At temperatures ranging from 150 ºC to 600 ºC, the weight loss was attributed to evaporation and decomposition of the organic moieties deposited. In general, it is described that the weight loss occurs mainly in two uneven stages, attributed to weakly and strongly bound alkyltriethoxysilanes. The first step takes place from *ca.* 150 to 375 ºC and corresponds to vaporization of physisorbed and hydrogen-bonded silanol molecules. The decomposition of strongly bounded species (highly cross-linked and/or chemisorbed silanes) by cleavage of C-C and Si-C bonds occurs in a second step in the range of *ca.* 375-600 ºC [25-27].

Polar mesoporous substrates have a highly reactive surface with a hydroxyl surface density of 4-6 $OHnm^{-2}$ [28]. In consequence, SB samples lost most of the deposited silane (80 %) in the second temperature stage of the thermograph (375-600 ºC). The maximum rate of thermal decomposition occurred at *ca.* 550 ºC. The mesoporous space facilitated the siloxane self-condensation reaction between adjacent silanols and the high hydroxyl surface density assisted the chemisorption, thus, resulting in highly stable coatings. TGA estimated amount of deposited silane in the interval 150-600 ºC was transformed using the BET surface area ($S_a$) to silane grafting density ($\rho_{grafting}$) expressed as the number of silane molecules per square nanometer [$m_s nm^{-2}$]. The estimated grafting densities for SB samples was *ca.* 1.0 $m_s nm^{-2}$. As reported in the literature, the maximum bonding density attained for small-pore silica gel substrates is 1.6 $m_s nm^{-2}$ when working at P > 500 bar [12]. The decrease of grafting density with respect to maximum was attributed to steric constrictions for molecules inside narrow irregular pores.

A continuous decay in the thermograph curve was observed for microporus zeolite samples in the range 200-600 ºC (Fig. 2b), with no inflexion point in the derivative curve. The surface density of silane deposited was 1.0 - 1.1 $m_s nm^{-2}$. Most of the weight loss (*ca.* 75-80 %) occurred in the low temperature range (200-375 ºC). For microporous samples, cross-linking is sterically hindered due to the lack of space, which resulted in a high number of low molecular weight species with low evaporation temperature. Moreover, silanol groups in zeolites were mostly present in the external surface as terminal groups, thus being difficult to attain chemisorption in the internal crystalline porous structure.

## Structural characterization

The FTIR spectra of the pristine matrices showed intense absorption bands in the 1000–1400 $cm^{-1}$ region, which corresponded to the stretching vibrations of the O–Si–O bond in the $SiO_4$ tetrahedrons of the $SiO_2$ skeleton. The band at *ca.* 950 $cm^{-1}$ was associated with vibrations of Si-OH bond. The two intense absorption bands present at 3400 and 1620 $cm^{-1}$ were assigned, respectively, to the stretching and deformation vibrations of adsorbed water molecules. The presence of silane coating in the prepared samples was confirmed by FTIR (Fig. 3) [29]. Characteristic bands corresponding to the organic part of the silane molecule were those appearing at *ca.* 2955 $cm^{-1}$ ($CH_3$ symmetric stretching), 2928-2914 $cm^{-1}$ ($CH_2$ antisymmetric stretching) and 2851 $cm^{-1}$ ($CH_2$ symmetric stretching).

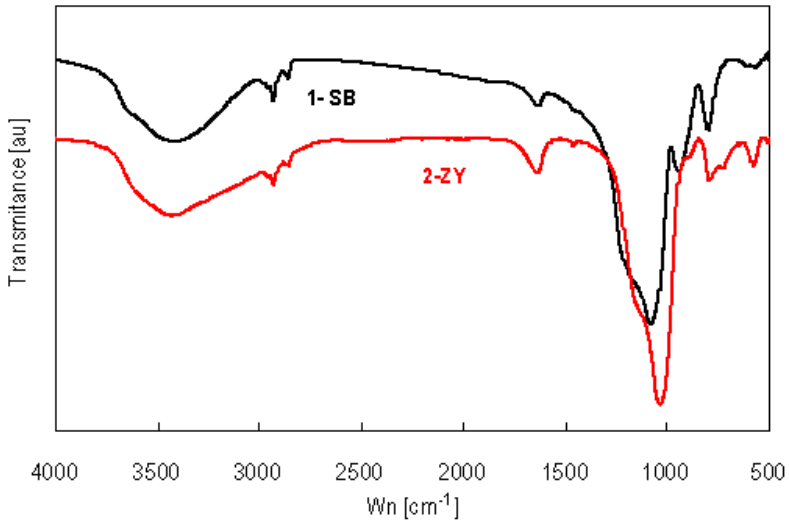


**Figure 3.** FTIR spectra of different impregnated matrixes.

## Textural properties

The decrease in surface area was more noticeable for substrates with microporosity, such as SB and ZY (Table 2). The thickness of the deposited $C_8SiO$- layer was estimated to be *ca.* 1.2 nm. As a consequence, silane deposition modified considerably the architecture of the cylinders with the smallest pore diameter, which had the highest contribution to the specific surface area. Similarly, the deposition of silane molecules on the internal surface of porous materials implied a decrease in pore volume, attributed to both decrease in mean pore diameter and potential pore blocking, more significant for materials with micropores.

## Water uptake

The treatment of the silica materials with silane was expected to confer hydrophobicity to the samples. A preliminary test on the hydrophobic behavior of the silanized material was performed by placing a water droplet on the surface of untreated powder wafers of compacted and silanized SB. It can be observed that for the wafer of untreated material, the contacting angle of water was initially less than 30º (Fig. 4a) indicating a hydrophilic material. On the contrary, for the silanized wafer, the water droplet on the top of the surface had a contact angle greater than 90º (Fig. 4b) showing its hydrophobic character.

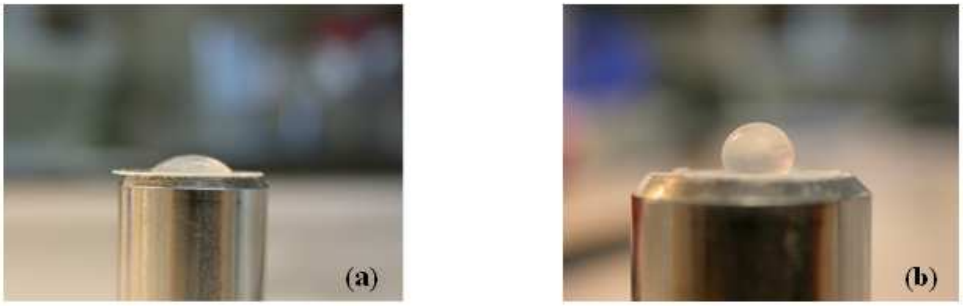


**Figure 4.** Water droplet over powder compacted wafer of: (a) untreated sample b-SB, and (b) silanized sample 2-SB.

In the SB samples, the modification of the water adsorption capacity was evidenced qualitatively from the color change of the moisture indicator (0.5-1 wt% cobalt chloride impregnated in the SB) from blue (dry) to pink (moisturized). As shown in Fig. 5, after 1 h of moisture adsorption under ambient conditions, the pink color was more evident for blank than for treated samples and the persistence of blue color increased with the processing time from 90 to 420 min.

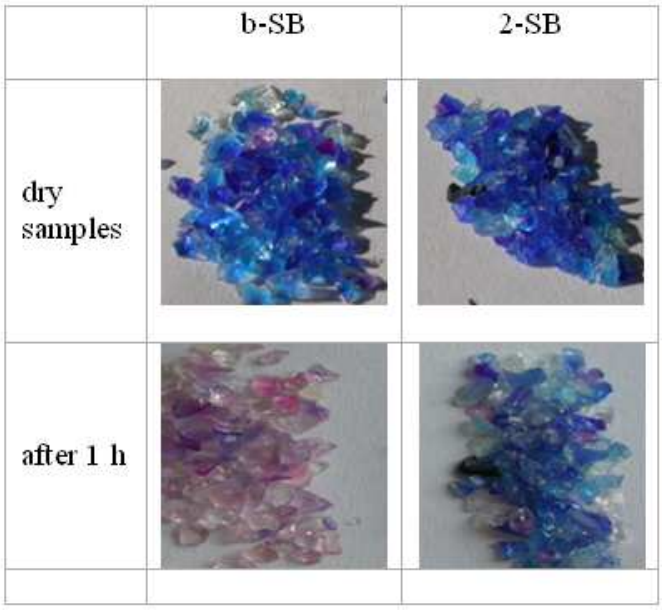


**Figure 5.** Optical pictures showing the modification of the color of silica blue samples from blue (dry) to pink (water saturate) by exposing them to a relative humidity of 64 % at 21 ºC.

In this work, the determination of water adsorbed using the Karl Fischer method was used to evaluate the hydrophobicity acquired by treated samples. Some samples were hydrated under ambient conditions during one week (Table 2) and the water desorption kinetics were then studied (Fig. 6). The percentage of water uptake for mesoporous samples was reduced to *ca.* 50% after silanization. Water adsorption drop was less important for microporous zeolite samples than for mesoporous matrices. For amorphous mesoporous silica, residual uncondensed hydroxyl groups from the original polymeric silicic acid remained on the surface of each primary silica particles, conferring upon silica gel its polar properties. Hence, the replacement of some Si–OH groups by hydrolytically stable (chemisorption) $C_8Si$- hydrophobic groups prevented, in part, water penetration. On the other hand, the zeolite is a crystalline hydrated aluminosilicate whose framework structure encloses cavities occupied by water molecules linked to the surface by electrostatic forces. Silane physisorption in such a pore network did not prevent effectively the adsorption of polar water.

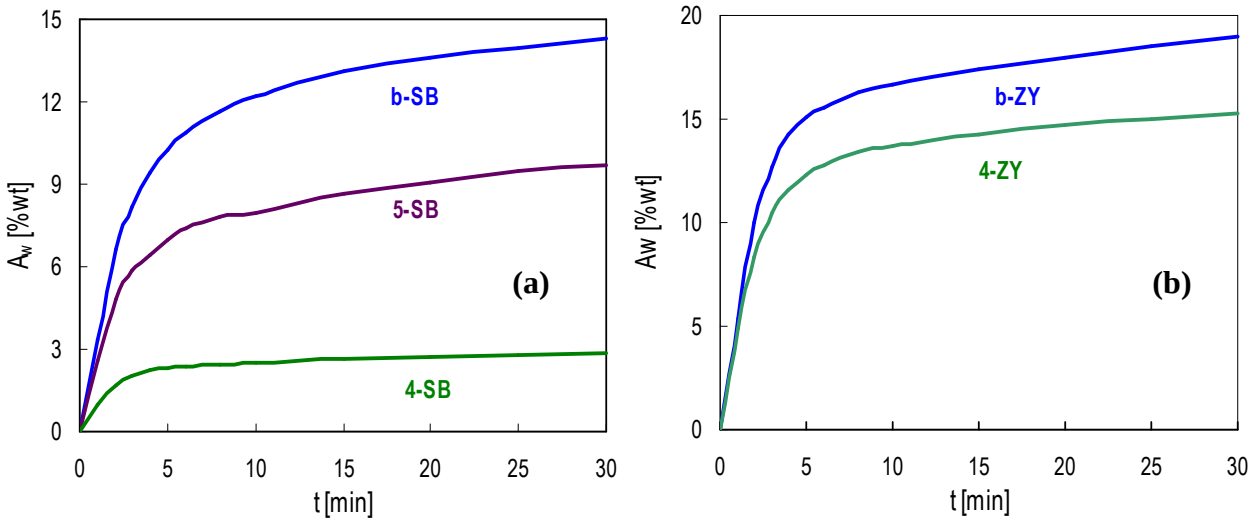


**Figure 6.** Curves of desorbed water, obtained using the Karl Fischer analytical method, from meso and microporous blank and silanized selected samples after hydration during one week: (a) SB, and (b) ZY.

## CONCLUSIONS

The silanization of silica meso and microporous substrates with a hydrophobic alkylsilane in $scCO_2$ has been investigated. The effectiveness of the supercritical process at 100-200 bar and 45-75 ºC was confirmed by means of the presence of a polysiloxane network, according to the ATR-FTIR spectrum of the silanized samples. TGA indicated that higher grafting densities were obtained in microporous substrates than in mesoporous materials. However, chemisorption was the dominant process found in mesoporous substrates, while physical deposition was the behavior observed for microporous matrices. Similarly, the percentage of water uptake was considerably reduced only for mesoporous samples after silanization.

**ACKNOWLEDGEMENTS**

The financial support of the Spanish government under projects Ingenio 2010 CEN-20081027 (CDTI) and CTQ2008-05370/PPQ, MAT2010-18155 is gratefully acknowledged. Additional support for this work has been provided by the Generalitat of Catalonia under project 2009SGR-666 and by Carburos Metálicos.

**REFERENCES:**

[1] ULMAN, A., Chem. Rev., 96, **1996**, 1533.
[2] EHLERT, N., MÜLLER, P. P., STIEVE, M., BEHRENS, P., Microporous Mesoporous Mater., 131, **2010**, 51.
[3] PLUEDDEMANN, E. P., Plenum Press New York, **1991**.
[4] SMITH, M. B., EFIMENKO, K., FISCHER, D. A., LAPPI, S. E., KILPATRICK, P. K., GENZER, J., Langmuir, 23, **2007**, 673.
[5] ANAC, I., MCCARTHY, THOMAS. J., J. Colloid Interface Sci., 331, **2009**, 138.
[6] BRITT, D. W., HLADY, V., Langmuir, 15, **1999**, 1770.
[7] DOMINGO, C., LOSTE, E., FRAILE, J., J. Supercrit. Fluids, 37, **2006**, 72.
[8] FADEEV, A. Y., MCCARTHY, T. J., J. Am. Chem. Soc., 121, **1999**, 12184.
[9] LAZGHAB, M., SALEH, K., GUIGON, P., AIChE J., 54, **2008**, 897.
[10] MARCINKO, S., HELMY, R., FADEEV, A. Y., Langmuir, 19, **2003**, 2752.
[11] WANG, Y.LIEBERMAN, M., Langmuir, 19, **2003**, 1159.
[12] CAO, C., FADEEV, A.Y., MCCARTHY, T. J., Langmuir, 17, **2001**, 757.
[13] GU, W.TRIPP, C. P., Langmuir, 22, **2006**, 5748.
[14] SHIN, Y., ZEMANIAN, T. S., FRYXELL, G. E., WANG, L. Q., LIU, J., Microporous Mesoporous Mater., 37, **2000**, 49.
[15] STOJANOVIC, D., ORLOVIC, A., GLISIC, S. B., MARKOVIC, S., RADMILOVIC, V., USKOKOVIC, P. S., ALEKSIC, R., J. Supercrit. Fluids, 52, **2010**, 276.
[16] TRIPP, C. P., COMBES, J. R., Langmuir, 14, **1998**, 7348.
[17] ZEMANIAN, T. S., FRYXELL, G. E., LIU, J., MATTIGOD, S., FRANZ, J. A., NIE, Z., Langmuir, 17, **2001**, 8172.
[18] GARCÍA-GONZÁLEZ, C. A., FRAILE, J., LÓPEZ-PERIAGO, A., DOMINGO, C., J. Colloid Interface Sci., 338, **2009**, 491.
[19] GARĆIA-GONZÁLEZ, C. A., SAURINA, J., AYLLÓN, J. A., DOMINGO, C., J. Phys. Chem. C, 113, **2009**, 13780.
[20] LOSTE, E., FRAILE, J., FANOVICH, M. A., WOERLEE, G. F., DOMINGO, C., Adv. Mater. (Weinheim, Ger.), 16, **2004**, 739.
[21] DASH, S., MISHRA, S., PATEL, S., MISHRA, B. K., Adv. Colloid Interface Sci., 140, **2008**, 77.
[22] MA, Y., TONG, W., ZHOU, H., SUIB, S. L., Microporous Mesoporous Mater., 37, **2000**, 243.
[23] WAGH, P. B., INGALE, S. V., GUPTA, S. C., J. Sol-Gel Sci. Technol., 55, **2010**, 73.
[24] GARCÍA-GONZALEZ, C. A., FRAILE, J., LOPEZ-PERIAGO, A., SAURINA, J.DOMINGO, C., Ind. Eng. Chem. Res., 48, **2009**, 9952.
[25] GARCÍA-GONZÁLEZ, C. A., ANDANSON, J. M., KAZARIAN, S. G., DOMINGO, C., SAURINA, J., Anal. Chim. Acta, 635, **2009**, 227.

[26] SEVERIN, J.W., CAMPS, I. G. J., BAKEN, J.M.E., VANKAN, J.M.J., Surf. Interface Anal., 19, **1992**, 133.
[27] MCELWEE, J., HELMY, R., FADEEV, A. Y., J. Colloid Interface Sci., 285, **2005**, 551.
[28] MUELLER, R., KAMMLER, H. K., WEGNER, K., PRATSINIS, S. E., Langmuir, 19, **2003**, 160.
[29] LIU, Y., YANG, R., YUM, J., WANG, K., Polym. Compos., 23, **2002**, 28.